International Journal of Engineering

Journal Homepage: www.ije.ir

Analysis Randon Causes Repeatability Errors Inducted by Friction at Joints in Industrial Robots

A. Rezala*[a,b], M. Arbaoui[a]

[a] *Department of Transport and Hydrocarbons Equipment, Hydrocarbons and Chemistry Faculty, University of M'hamed Bougara -Boumerdes (UMBB), Boumerdes, Algeria*
[b] *Department of Mechanical and Production Engineering, Mechanical and Process Engineering Faculty, University of Science and Technology Houari Boumediene (USTHB), BP 32 El Alia 16111 Bab Ezzouar Alger, Algeria*

PAPER INFO

Paper history:
Received 30 September 2021
Received in revised form 26 November 2021
Accepted 08 December 2021

Keywords:
Repeatability
Friction
Asperity
Industrial Robot

ABSTRACT

The present study was carried out to investigate and analyze the positionning repeatability introduced by friction variations based on stochastic ellipsoids. A mixed friction model has been developed with improved properties compared to existing standard models. The contact is presented as a multitude of micro contacts whose nature can be of two types: lubricated and solid. This model is experimentally tested on a reciprocating tribometer under extreme friction conditions, with sliding speed varying from 0.1 to 3 m/s and load modified from 40N to 150N to discuss the effect of speed, the effect of nominal contact pressure and the effect of sliding distance on friction parameters. The results showed how this model can be represented as a sum of functions of the relevant states, which are linear and nonlinear in the friction parameters. Thus, these results were used to evaluate the covariance matrix in order to locate the different ranges of errors which have an impact on the repeatability of position.

doi: *10.5829/ije.2022.35.02b.21*

1. INTRODUCTION

Lately, robotic systems have been progressively carried out many engineering applications [1-3] to replace humans in simple, repetitive and dangerous tasks. In order to optimize trajectory planning, we can use the criteria of energies [4, 5] position as well as speed and acceleration. The criterion of energy consumption as in the transport and handling of industrial objects depends on the robots used as mobile robot or manipulator. The work in this case takes into account the aerodynamics of the robot (dynamic model) [5]. This part consists of optimizing the pneumatic energy. The phenomenon of abrupt change of orientation using continuous movement in position and tangent (first and second-degree continuity) is detrimental for the assembly. The trajectory planning discussed by Wan et al. [6] has determined by an initial starting point Pi as well as its arrival at the final point Pf, avoiding to collision phenomenon. This would require recording the position and orientation of a set of points. Then approximate by a curve (using Bezier, B-Splines and NURBS). Other authors translate the phenomenon by a description of an object gripper of different shapes as well as the functioning of the gripper jaws [7]. Another method of describing objects of complex shapes using a set of 3D points has been developed in order to position and orient these complex points [8].

The absolute precision of an industrial robot is affected by systematic errors, in which the causes are generally known and can be easily compensated by corrective actions during calibration. However, repeatability is usually affected by errors of a random nature, caused by the adjustments of the servo-controls and especially by non-geometric phenomena such as hysteresis, play and friction existing at the joints [9] difficult to model and not permanently compensating for precisely because of their random nature. For this reason,

*Corresponding Author Institutional Email: a.rezala@univ-boumerdes.dz (A. Rezala)

Please cite this article as: A. Rezala, M. Arbaoui, Analysis Randon Causes Repeatability Errors Inducted by Friction at Joints in Industrial Robots, ***International Journal of Engineering, Transactions B: Applications***, Vol. 35, No. 2, (2021) 451-457

repeatability is considered to be one of the most important specifications to consider when selecting a robot. The repeatability error quantifies the level of spatial dispersion of the programmed pose of a robot. This is a very important metrological characteristic of an industrial robot. There are many recommendations for modeling and calculating the repeatability of industrial robots. Among the most commonly used methods, we will retain the stochastic ellipsoid method [10] the Taguchi method (signal/ noise ratio), and the method of the ISO 9283 standard [11].

One of the major difficulties in the robotics is friction, therefore, the analysis of friction in the robot joint is an important topic in tribology and industrial robotics. The main issue with mechanical systems in industrial robots is the friction caused by complicated and multiple sets of microscopic interactions between surfaces that are contact and slide. These interactions are the result of the physic-chemical properties of the materials, the geometrical and topographical characteristics of the surfaces and the overall conditions under which the surfaces are made to slide against each others [12]. Therefore, friction is not simply a property of materials parameters; it is unique characteristics of the tribological system in which it is measured. In the design of an industrial robot, friction management is a permanent challenge [13]. Friction has been widely studied by many scientists, due to its importance in several areas of mechanical engineering. Uncompensated friction occurring at the joints level causes of non negligible positioning errors on the accuracy of the robot's terminal organ. Thus, the presence of friction at joints constitutes one of the main causes of performance loss in manipulator since the friction is a source of the deviations in poses causing of defect repeatability. But, the friction modeling is not an easy task then it is too difficult to expect its correction. Hence, the interest in seeking precise modeling of friction behavior requires a model of friction forces, which based on the real behavior of joints.

The main objective of present study is to study and analyze the repeatability of position induced by friction variations, using a probabilistic approach based on stochastic ellipsoids. This approach makes it possible to better characterize the repeatability of the robot at each point of its workspace and thus better plan its tasks. Therfore, a numerical model analysis of the mixed friction behavior of the components of the robot joints was used. This model is based on an analysis of the contact geometry and it is confronted with an experimental study by equivalent geometric model, in a lubricated medium, on an alternative tribometer in extreme conditions of friction, with a sliding speed varying from 0.1 to 3 m/s and a modified load from 40N to 150N to discuss the effect of speed, the effect of nominal contact pressure and the effect of sliding distance on friction parameters.

2. COMPARISON BETWEEN NUMERICAL AND REAL APPLICATION

In our work, we used a structure working in the 3D coordinate systemin translation including a gripper. It is of great interest for transfer operations. This structure is widely used in conditioning applications since in these applications the three translations are sufficient. A rotational movement along the z-axis is often added to the terminal organ.

The robot is designed by three joints with one degree of freedom each. Therefore, the positioning error is divided into three to ensure the positioning accuracy at the output of the terminal organe. In other words, the positioning repeatability is determined at the end of the segment. The proposed joint is a sliding link with one degree of freedom. It is real when it is driven by an engine, reducer, screw/nut and the movable part called the segment, which moves relative to the fixed part generally linked to the built called the slide (or guide). An schematic diagram of kinematic for a slide link attached to the terminal organe is shown in Figure 1.

The proposed kinematic link can be schematized by two bodies junction for complementary functions. The first body consists of transmission mechanism; engine-slide. A rigidity of spring k can idealize this part. The second body corresponds to the segment-slide part. An alternative translation tribometer can symbolize the latter. Therefore, the sources of errors request the repeatability dispersion, that can be devided into two parts. The first one brings together all mechanical and geometric errors (alignment, vibration, force and adjustment), while the second one contains the friction and wear errors (friction coefficient, mechanical games and energy loss). Therefore, the proposed kinematic link can be revealed by Figure 1, where it is detailed in the tribological part Segment-slide of the link, which proposed by a contact Pin-plate from the alternative tribometer to idealize the movement and simplify the positioning of the effector (output element). In addition, it is assumed that the mechanical contribution (elasticity of the spring) to the positioning repeatability is constant. While, the positioning repeatability only depends on the variation force or the coefficient friction and wear that appears

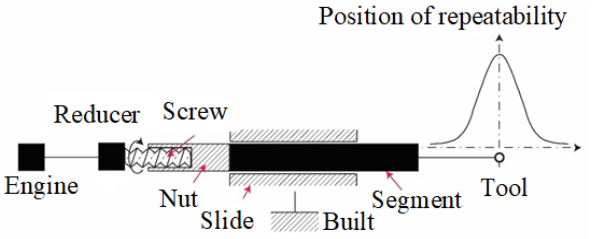

Figure 1. Kinematic diagram of a slide link attached to the terminal organe

between segment and slide, consequently the quantification of the tribological error on the positioning repeatability. The validation of experimental data an alternative tribometer is used as shown in Figure 2.

3. EXPERIMENTAL PROCEDURE

Alternative tribometer was produced and designed in Laboratory of Mechanical Structures and Materials Engineering (LISMMA), in Paris, was utilized to perform tribo test as seen in Figure 3 to study the work in progress at medium nominal contact pressure (up to12 Mpa), high sliding speed (up to 10 m/s) and normal load (up to 500 N).

The test pieces used on the tribometer are a plate representing a steel slide 42CD4 and a pin representing a segment made of 100C6 steel are shown in Figure 4.

Sliding tests were carried out at room temperature, with sliding speed in the span of 0.1-3 m/s and the load were changed from 40 N to 150 N. To ensure that the two rubbing surfaces make excellent, consistent contact, rubbing of segment specimens was carried out with a

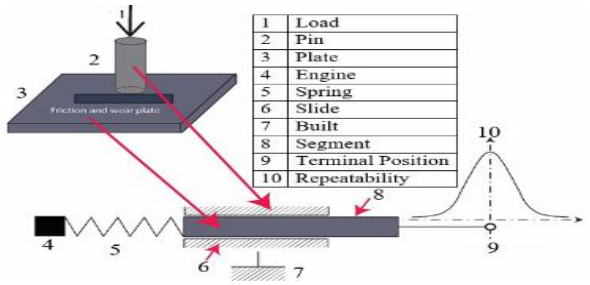

Figure 2. Experimental validation on an alternative tribometer

Figure 3. Alternative tribometer used

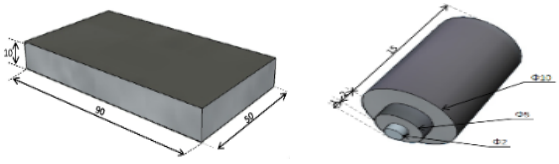

(a) (b)

Figure 4. Test simples : (a) Plate, (b) Pin

silicon abrasive paper before the tests. i. e. contacting surfaces. The frictional force was measured using a strain gauge present at the level arm that holds the specimen. The coefficient of friction value was calculated using the ratio of frictional force to normal load. After calculation, we were able to determine the speed error, which amounts to plus or minus 1%, as well as the load error, which is 0.05 mv.

4. CONSTITUTION OF A MIXED FRICTION MODEL

4. 1. Qualitative Analysis The diagram below shows that micro geometry plays a key role in lubrication, it constitutes the first stage of the modeling developed in the digital tool. We will adopt a circular approximation for the shape of asperities. Then, it is necessary to define the fraction of force α passing through the contacts working in thin film, the remainder 1-α corresponding to forces passing through the contacts working in thick film. We put f_s the coefficient of friction on the thin film contacts and f_l the coefficient of friction of the thick film contacts. We naturally have $f_s > f_l$. The total friction f is defined by the expersion below:

$$f = \alpha f_s + (1-\alpha) f_l \tag{1}$$

This justifies the name of mixed friction. The digital tool used makes it possible for a given situation to calculate α and therefore to deduce f from it by giving ourselves f_s and f_l.

4. 2. Modeling of Micogeometry The micro geometry is approximated by a succession of roughness of vertices spaces of AR whose vertices follow a normal law with mean R/2 and standard deviation:.

$$p_1(z) = \frac{1}{SAlt\sqrt{2\Pi}} \exp\left[-\frac{1}{2}\left(\frac{z-Alt}{SAlt}\right)^2\right] \tag{2}$$

where

$$SAlt = 0.35\sqrt{W^2 + SW^2}$$
$$Alt = \frac{1}{2}R \tag{3}$$

where $P_1(z)$ is statistical distribution of peak altitude; z is summit altitude of asperity; and Alt and SAlt are mean and root mean square of the peak altitude.

The radii of the asperities follow a lognormal distribution whose characteristics also depend on roughness parameters. The lognormal distribution is given by the following formula instead of a classical normal distribution:

$$p_2(R^*) = \frac{1}{aR^*\sqrt{2\Pi}} \exp\left[\frac{1}{2a^2}\left(\log R^* - b\right)^2\right] \tag{4}$$

where R* is a dimensional expression of radius R; R is the radius of asperity; a and b are constants for radius distribution. This lognormal distribution is available only for the positive values and requires a dimension less parameter R*.

$$R^* = \frac{R}{SRAD} \tag{5}$$

4. 3. Modeling of the Contact Between Segment-slide of the Robot For a given position d counted from the mean line, it will be considered that the asperities whose vertices have an altitude z greater than d working in thin film with a friction f_s while those having an altitude z less than d working in thick film (coefficient of friction f_l).

The value d physically corresponds to the average thickness of the lubricant. Knowing the expressions of the behavior of each of these families of asperities (force on an asperity according to the crushing), it is possible to numerically determine the total coefficient of friction of the contact and the total loading which it undergoes. The model takes into account the deformations: elastic, elastoplastic, plastic, elastohydrodynamic and hydrodynamic of the asperities in contact. For roughness [14] working in thick film lubrication regime, mechanisms such as hydrodynamics with piezo-viscous effect and elastohydrodynamic were analyzed. Figure 5 depicts the description of the modelling of the contact between segment-slide of the robot.

The total friction f is defined by Equation (6):

$$\begin{aligned} W &= \sum W_E + \sum W_{EP} + \sum W_P + \sum W_{PVR} + \sum W_{EHD} \\ F &= \sum F_E + \sum F_{EP} + \sum F_P + \sum F_{PVR} + \sum F_{EHD} \\ \Rightarrow f &= F/W \end{aligned} \tag{6}$$

In this case, the proposed mixed friction model is represented by a sum of functions of the relevant states, which are linear and nonlinear in the friction parameters.

5. RESULTS AND DISCUSSION

5. 1. Result Obtained by the Model The results of friction coefficient calculation as a function of the Sommerfeld number, defined by the defined equation S = ηV/ p where η represents the viscosity, U is the sliding speed and p is the apparent pressure are shown in Figure 6.

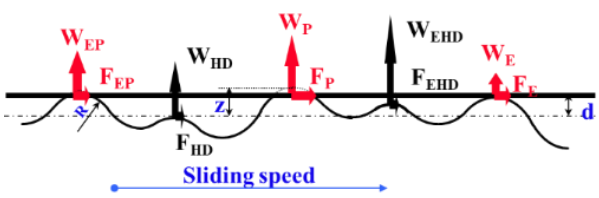

Figure 5. Description of the modelling

The results of calculation of the coefficient of friction followed the typical shape of the curve of Stibeck [15] where one notes a dispersion of the values of the coefficient of friction which is due to two types of lubricated and solid contact. The lubricated contact where there is a continuous film, with well separated bearing surfaces, the lubrication is in HD or EHD regime and the friction is viscous equal to approximately 0.004. The asperities are not in contact and therefore, the load is supported by the fluid. In addition, a solid contact where there is a discontinuous film and where tangential actions can occur due to the proximity of the bearing surfaces of the same nature as those which determine the solid friction. The lubrication is in mixed regime and the friction is coupled: viscous and solid equal to approximately 0.1, the asperities are in direct contact and therefore, the load is partly supported by the latter.

5. 2. Experimental Validation on an Alternative Tribometer This model is tested by the experiments carried out on the reciprocating tribometer. For each of these tests, we used the friction coefficient values.

By superimposing the curves obtained from the model illustrated in Figure 6 and the experimental data we obtained for the friction coefficients are illustarted in Figure 7, which combined the two experimental and theoretical predicted results by modelling.

5. 3. Discussion: Model-experiment Comparison A slight difference is observed between the experimental results and the model, for the value of the coefficient of friction on the contrary to the existing standard models This can be explained by imperfections in the model, and/or by those when performing the experiments.

The first approximation is erroneous because the distribution of contacts is considered not equal between all the types of micro switches: that is to say that there are not as many segment-slide contacts and this, at the level of the real contact area. The actual contact shown schematically in Figure 5 shows that this hypothesis is not

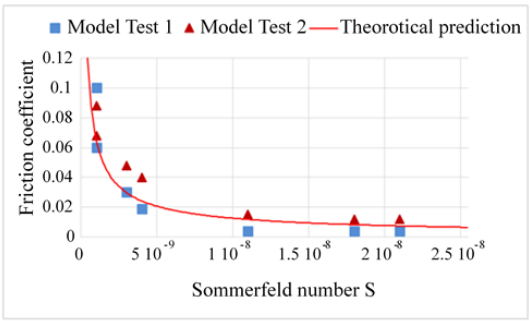

Figure 6. Friction coefficients determined by the model with respect to Sommerfeld number

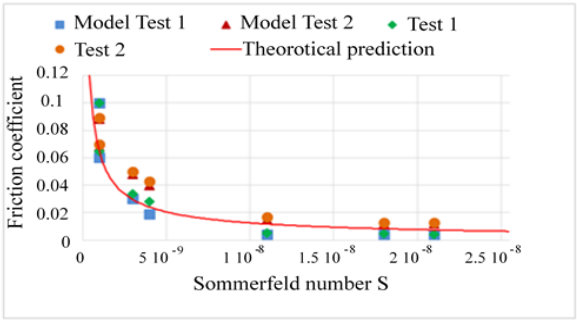

Figure 7. Comparaison of experimental and calculated friction coefficients as a function of S

valid because the radii of the asperities follow a lognormal distribution whose characteristics also depend on roughness parameters such as the average height of the roughness pattern R, the standard deviation of the pattem heights SR, the average width of the roughness pattem AR , the standard deviation of the SAR pattern widths, the mean height of the W ripple pattern, and the standard deviation of the SW ripple pattern heights. Thus, the surfaces are described by a statistical distribution function of peak altitude and asperities radius where the density function of the probability is illustrated in Figure 8, which is defined by the following equation:

$$p(z,R) = p_1(z) \cdot p_2(R) \quad (7)$$

To illustrate this analysis in a suitable manor, Figure 9 presents by level curves, shown as a Gaussian distribution of the heights of asperities as a function of their radii of curvature.

The second assumption of the model is the isotropy of the tribological properties. Although the steel is statically isotropic, that is to say on a macroscopic scale, the steel exhibits a strong anisotropy at least in terms of mechanical properties.

5. 4. Wear Figure 10 illustrates the evolution of the wear coefficient K as a function of Sommerfeld

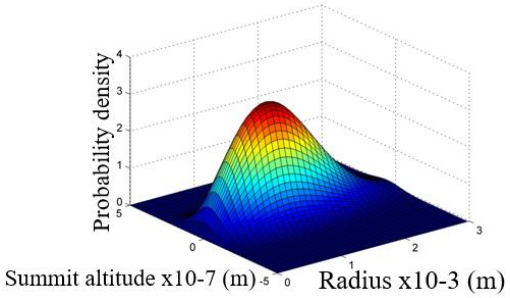

Figure 8. Density probability function of asperities as a function of radius and summit altitude

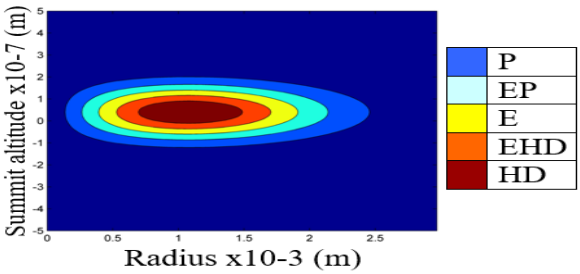

Figure 9. Gaussian distribution of the five types of asperities

number [16]. This is a complementary model to the wear Achard's law, which holds coccount of the dispersion induced by fluctuations in the characteristics of the microgeometries, from one contact area to another [17]. While, the Archard's law constitutes the major difficulty of a contact in a mixed lubrication situation. One of the assumptions of this Archard law is that the contact took place in a dry environment. In our study, the lubrication is mixed, therefore, Archard's law can be generalized on condition of taking into account the contact pressure supported by the non-lubricated asperities (in thick film). The wear process and its properties are studied on the basis of the mixed friction observed in the joint of an industrial robot, where it can be concluded that the dispersion observed in the results obtained is generated by variable lubrication conditions, the friction coefficient of which varies between 0.004 and 0.1.

The wear of peak altitude of the asperities due to the adaptation of the surfaces in the robot articulation can thus be used as an indicator of the state of the articulation and they cause considerable damage and constitute an excellent indicator of damage to the mechanical surfaces. Therefore, wear and tear processes can take several years to be significant, but can change rapidly once they start to appear. To conclude, the obtained results showed us that there is a proportionality between friction and wear in the joints of industrial robots.

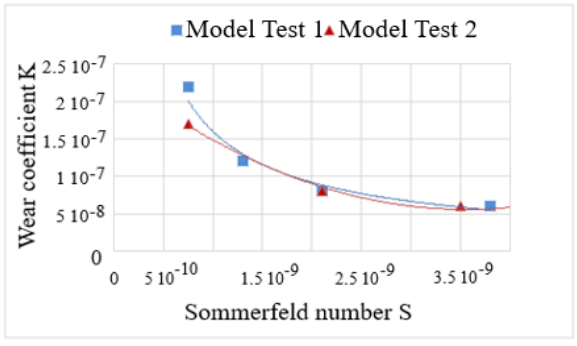

Figure 10. Evolution of wear coefficient K as a function of the Sommerfeld number

6. ANALYSIS RANDON OF THE POSE REPEATABILITY INDUCTED BY FRICTION

We made a simulation in a basic parallelepiped work volume (400 x 400 mm) in order to show the influence of friction on the field calculation of the organ's positioning repeatability of the robot terminal. Figures 11, 12 and 13 show the horizontal sections. It can be seen that the errors in the plane presented in Figure 11, show that the point cloud is located in an ellipsoidal zone where the limitation adopted on the joints has shown its effectiveness. This is due to the friction which is minimal, because we are in a situation of thick film lubrication. In this case, the friction results from a partition of the contact, the positioning of the terminal member of which is almost precise.

Indeed, beyond the limited working space, there is a significant increase in the positioning error of the terminal member of the robot illustrated in Figures 12 and 13. These figures also show that the friction is due in a significant way to the gap existing between the segment and the slide. In particular, for the high values of friction which resulted in from a partition of the contact in the thin film. By analyzing these graphs, we observed that by iteration, our robot performs a maximum error at the center of the plane perpendicular to the displacement. This error is mainly caused by the friction.

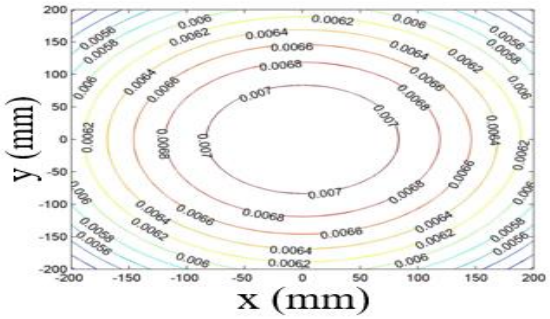

Figure 11. Repeatability field in µm at the plane z = - 400 (mm)

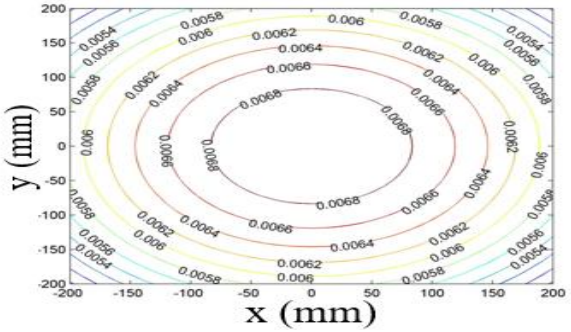

Figure 12. Repeatability field in µm at the plane z = - 500 (mm)

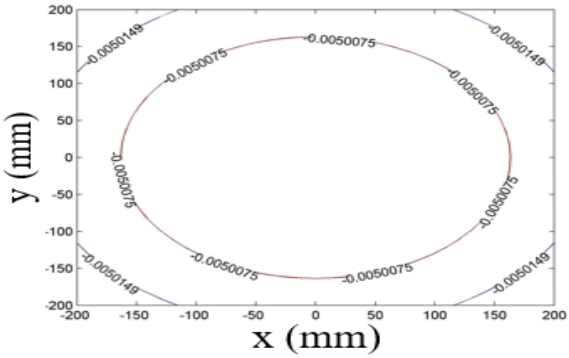

Figure 13. Repeatability field in µm at the plane z = - 600 (mm)

7. CONCLUSION

This research study presents the results and statistical analyses of a study devoted to the estimation of positioning repeatability induced by friction variations. The theory of stochastic ellipsoids has been used to describe the spatial distribution of workspace errors around the mean position where the results are graphically visualized. This model allowed us to choose the best location in the workspace to perform the task. The findings of this research and evaluation are listed below:

- The absolute value of the error made on the computation of repeatability is lower than 2.10^{-3}. This value of the calculated repeatability is considered acceptable.
- The repetitive positioning of the robot's terminal organ follows a normal distribution around the commanded position.
- The level of dispersion decreases as a function of time (asymptotic behavior) to reach its lowest value, then stabilizes at an almost constant value;
- In the plane z = -400 mm, the point cloud is located in an ellipsoidal zone where the friction is equal to 0.004,
- For high values of friction, there is an increase in the positioning errors of the terminal organ.
- The results obtained by the model of mixed friction in qualitative and quantitative adequacy with the experiment.
- The mixed friction model takes into account the roughness parameters, the nature of the materials, the lubricant, the forces and the speeds.

8. REFERENCES

1. Tang, G., Webb, P., Thrower, J.J.R. and Manufacturing, C.-I., "The development and evaluation of robot light skin: A novel robot signalling system to improve communication in industrial human–robot collaboration", ***Robotics and Computer-Integrated***

Manufacturing, Vol. 56, (2019), 85-94, doi: 10.1016/j.rcim.2018.08.005

2. Khorashadizadeh, S. and Fateh, M.M.J.R., "Uncertainty estimation in robust tracking control of robot manipulators using the fourier series expansion", Vol. 35, No. 2, (2017), 310-336, doi: 10.1017/S026357471500051X
3. Sangdani, M. and Tavakolpour-Saleh, A.J.I.J.o.E., "Parameters identification of an experimental vision-based target tracker robot using genetic algorithm", ***International Journal of Engineering, Transactions C: Aspects,*** Vol. 31, No. 3, (2018), 480-486, doi: 10.5829/ije.2018.31.03c.11
4. Savkiv, V., Mykhailyshyn, R., Duchon, F. and Mikhalishin, M.J.J.o.E.E., "Energy efficiency analysis of the manipulation process by the industrial objects with the use of bernoulli gripping devices", ***Journal of Electrical Engineering,*** Vol. 68, No. 6, (2017), 496, doi: 10.1515/jee-2017-0087
5. Mykhailyshyn, R., Savkiv, V., Mikhalishin, M. and Duchon, F., "Experimental research of the manipulatiom process by the objects using bernoulli gripping devices", in 2017 IEEE International Young Scientists Forum on Applied Physics and Engineering (YSF), IEEE. (2017), 8-11.
6. Wan, W., Igawa, H., Harada, K., Onda, H., Nagata, K. and Yamanobe, N.J.A.R., "A regrasp planning component for object reorientation", Vol. 43, No. 5, (2019), 1101-1115, doi: 10.1007/s10514-018-9781-y
7. Savkiv, V., Mykhailyshyn, R., Maruschak, P., Kyrylovych, V., Duchon, F. and Chovanec, Ľ.J.T., "Gripping devices of industrial robots for manipulating offset dish antenna billets and controlling their shape", Vol. 36, No. 1, (2021), 63-74, doi: 10.3846/transport.2021.14622
8. Wermelinger, M., Johns, R., Gramazio, F., Kohler, M., Hutter, M.J.I.R. and Letters, A., "Grasping and object reorientation for autonomous construction of stone structures", ***IEEE Robotics and Automation Letters***, Vol. 6, No. 3, (2021), 5105-5112, doi: 10.1109/LRA.2021.3070300
9. Deblaise, D., "Contribution à la modélisation et à l'étalonnage élasto-géométriques des manipulateurs à structure parallèle", INSA de Rennes, (2006),
10. Assoumou Nzue, R., Brethe, J.-F., Vasselin, E. And Lefebvre, D., "Comparaison de la répétabilité des robots manipulateurs sériels et parallèles à l'aide des ellipsoïdes stochastiques", in Congrès français de mécanique, AFM, Maison de la Mécanique, 39/41 rue Louis Blanc, 92400 Courbevoie, France, (2011).
11. Kumičáková, D., Tlach, V. and Císar, M., "Testing the performance characteristics of manipulating industrial robots", ***International Organization for Standardization*** (2016).
12. Al-Bender, F. and Swevers, J.J.I.C.S.M., "Characterization of friction force dynamics", ***IEEE Control Systems Magazine*** Vol. 28, No. 6, (2008), 64-81, doi: 10.1109/MCS.2008.929279
13. Bona, B. and Indri, M., "Friction compensation in robotics: An overview", in Proceedings of the 44th IEEE Conference on Decision and Control, IEEE. (2005), 4360-4367.
14. Venkata Vishnu. A and Sudhakar Babub. S, "Mathematical modeling and multi response optimization for improving machinability of alloy steel using rsm, grey relational analysis and jaya algorithm", ***International Journal of Engineering, Transactions C: Aspects***, Vol. 34, No. 09, (2021), 1257-1266, doi: 10.5829/ije.2021.34.09C.13
15. Belarifi, F., Blouet, J., Inglebert, G., Benamar, A.J.M. and Industry, "Confrontation d'un modèle théorique en lubrification mixte avec une étude expérimentale du comportement au frottement d'une denture d'engrenage droit", Vol. 7, No. 5-6, (2006), 527-536, doi: 10.1051/meca:2007010
16. Zailani. Z-A, R.N.S.N. and Shuaiba. N-A, "Effect of cutting environment and swept angle selection in milling operation", ***International Journal of Engineering, Transactions B: Applications***, Vol. 34, No. 11, (2021), 2578-2584, doi: 10.5829/ije.2021.34.12c.02
17. Robbe-Valloire, F., Progri, R., Paffoni, B. and Gras, R., "Prediction of wear rate dispersion in mixed lubrication", in World Tribology Congress. Vol. 42010, (2005), 453-454.

Persian Abstract

چکیده

مطالعه حاضر به منظور بررسی و تحلیل تکرارپذیری موقعیت‌یابی معرفی‌شده توسط تغییرات اصطکاک بر اساس بیضی‌های تصادفی انجام شد. یک مدل اصطکاک مختلط با خواص بهبود یافته در مقایسه با مدل های استاندارد موجود توسعه یافته است. کنتاکت به صورت انبوهی از میکرو کنتاکت ها ارائه می شود که ماهیت آنها می تواند دو نوع باشد: روغن کاری شده و جامد. این مدل به صورت تجربی بر روی یک تریبومتر رفت و برگشتی تحت شرایط اصطکاک شدید، با سرعت لغزش از ۰٫۱ تا ۳ متر بر ثانیه و بار تغییر یافته از ۴۰ نیوتن تا ۱۵۰ نیوتن برای بحث در مورد تأثیر سرعت، تأثیر فشار اسمی تماس و اثر لغزش آزمایش می‌شود. فاصله بر روی پارامترهای اصطکاک نتایج نشان داد که چگونه می توان این مدل را به صورت مجموع توابع حالت های مربوطه که در پارامترهای اصطکاک خطی و غیرخطی هستند، نشان داد. بنابراین، این نتایج برای ارزیابی ماتریس کوواریانس به منظور تعیین محدوده‌های مختلف خطاهایی که بر تکرارپذیری موقعیت تأثیر دارند، استفاده شد.